Atmósfera 39, 263-281 (2025)
https://doi.org/10.20937/ATM.53442

A quantitative study of extreme rainfall intensity and occurrence in northern Algeria

Ahmed KHELOUFI ATTOU*, Kamila BABA-HAMED and Abderrazak BOUANANI

Laboratory (No. 25), Promotion of Water, Mineral and Soil Resources, Environmental Legislation and Technological Choices, University of Tlemcen, BP 119, Tlemcen 13000, Algeria.
*Corresponding author; email: attou.kheloufi@univ-tlemcen.dz

Received: September 18, 2024; Accepted: January 13, 2025

RESUMEN

En este trabajo se examinan las características asociadas a la evolución espaciotemporal de las precipitaciones extremas, se evalúa su frecuencia de recurrencia y se predicen los futuros niveles de retorno sobre el norte de Argelia. El estudio emplea índices de precipitación extrema junto con la aplicación de la teoría de valores extremos a un conjunto de datos pluviométricos que abarcan de 1982 a 2022. El estudio se concentró en la modelización del índice que demostró el mayor porcentaje de tendencias positivas significativas al nivel de significancia $\alpha = 5\%$. Para ello se utilizaron la prueba de Mann-Kendall y la distribución del valor extremo generalizado. Posteriormente, el modelo se validó mediante la prueba de ajuste de Kolmogorov-Smirnov. Los resultados revelaron que la región nororiental de la zona de estudio presentaba un aumento más pronunciado de la intensidad de precipitaciones en comparación con las regiones meridional y occidental. Se observaron tendencias significativas en la intensidad de las precipitaciones a lo largo del tiempo. En particular, el índice de días con precipitaciones superiores a 20 mm presentó el mayor porcentaje de tendencias positivas, con un 88% de las estaciones meteorológicas mostrando una tendencia al alza. Además, se identificó una fuerte correlación entre el índice de días con precipitaciones superiores a 20 mm y el índice de días muy húmedos, particularmente en las mesetas altas y en la región occidental. Este hallazgo apoya la hipótesis de que los patrones de precipitaciones extremas son cada vez más frecuentes en la región.

ABSTRACT

This paper examines the characteristics associated with the spatiotemporal evolution of extreme precipitation, assesses its recurrence frequency, and predicts future return levels over northern Algeria. The study employs extreme precipitation indices in conjunction with the application of extreme value theory to a rainfall dataset spanning from 1982 to 2022. The study focused on modeling the index that demonstrated the highest percentage of significant positive trends at the $\alpha = 0.05$ significance level. This was accomplished through the utilization of the Mann-Kendall test and the generalized extreme value distribution. Subsequently, the model was validated using the Kolmogorov-Smirnov fit test. The results revealed that the northeastern region of the study area experienced a more pronounced increase in rainfall intensity compared to the southern and western regions. Significant trends in precipitation intensity were observed over time. Notably, the index of days with rainfall exceeding 20 mm demonstrated the highest percentage of positive trends, with 88% of meteorological stations exhibiting an upward trend. Furthermore, a strong correlation was identified between the index of days with rainfall exceeding 20 mm and the very wet days index, particularly in the high plateaus and western region. This finding supports the hypothesis that extreme rainfall patterns are becoming more frequent in the region.

Keywords: North Algeria, climate change, extreme rainfall, indices, R20mm.

1. Introduction

Extreme precipitation events are typically understood to have two contrasting aspects. The first is characterized by insufficient rainfall, which can lead to drought conditions. The second is marked by excessive rainfall, which can result in flooding, landslides, and other severe consequences. Both aspects can lead to significant damage to infrastructure, agriculture, and ecosystems. However, intense periods of rainfall also have the potential to restore arid landscapes, replenish river levels, and recharge reservoirs, making them an important component of the water cycle.

The role of climate change in altering weather patterns and increasing the frequency and intensity of extreme precipitation events is well-documented (Kanae et al., 2004; Nicholson et al., 2013; Clarke et al., 2022; Kim et al., 2023; Jiménez-Esteve et al., 2024). As global temperatures rise, atmospheric conditions are modified, leading to more frequent and intense rainfall events. Therefore, monitoring fluctuations in extreme precipitation is critical for disaster preparedness, risk mitigation, and the sustainable management of water resources across various spatial and temporal scales. Addressing these challenges requires comprehensive research and the formulation of informed policies (Knutson et al., 2020).

Understanding the historical evolution of extreme rainfall events and developing reliable projections of future trends are essential for effective planning and adaptation strategies. Detecting changes in rainfall extremes through climate statistics is more likely to yield significant insights than focusing solely on individual extreme events (Easterling et al., 2000). This objective can be achieved by leveraging a variety of data sources, including ground-based stations and satellite observations. Consequently, a substantial body of research is devoted to examining fluctuations in extreme weather phenomena, particularly the impact of climate change on global precipitation patterns (Asadieh and Krakauer, 2015; IPCC, 2021).

In the Mediterranean Basin, climate change is significantly altering precipitation patterns, resulting in a general decrease in rainfall and an increase in the frequency of extreme events. These changes have profound implications for agriculture, water resources, and risk management (Giorgi and Lionello, 2008). Algeria, located within this basin, experiences a Mediterranean climate that transitions gradually from semi-arid in the north to arid in the south. The eastern part of the country typically receives more precipitation than the western part (Meddi and Toumi, 2015; Azioune et al., 2023). Evidence suggests that Algeria is already experiencing the effects of climate change, including reduced annual precipitation, more frequent droughts, and a subsequent decrease in the rate of surface runoff (Ghenim et al., 2010; Laborde et al., 2010; Bendjema et al., 2019). Extreme precipitation events are also becoming more intense in Algeria (Taïbi et al., 2019; Seneviratne et al., 2021; Hamitouche et al., 2024a).

The present study contributes to the expansion of our understanding of heavy rainfall events in northern Algeria. It employs a novel analytical approach that has not previously been addressed in Algeria. The primary objective is to examine the spatial and temporal fluctuations in extreme rainfall indices in northern Algeria by using a modeling approach to an index that reflects the trends observed in the majority of the studied stations. The aim is to estimate the intensity of extreme rainfall events and their return levels, as well as to identify the regions exposed to this intensity.

2. Materials and methods

2.1 Materials

2.1.1 Study area

The study area focuses on the northern portion of Algeria (Fig. 1), which encompasses several key geographic regions, including the fertile coastal plains of Mitidja, Habra, and Cheliff. Additionally, the area encompasses the Tellian Atlas mountain range, which includes the Tessala, Beni Chougrane, Ouarsenis, and Kabylie mountains, as well as the Saharan Atlas Mountain range, comprising the Ksours, Amour, and Ouled Nail Mountains. The Algerian steppe, or high plateau, stretches between the Tellian Atlas to the north and the Saharan Atlas to the south.

These mountain ranges play a crucial role in shaping the region's climate diversity, contributing to the variability observed in precipitation patterns (Meddi and Meddi, 2009; Ghenim and Megnounif, 2016). The climate of northern Algeria varies across different regions. Coastal areas experience a Mediterranean climate, characterized by warm summers with average maximum temperatures around 30 ºC,

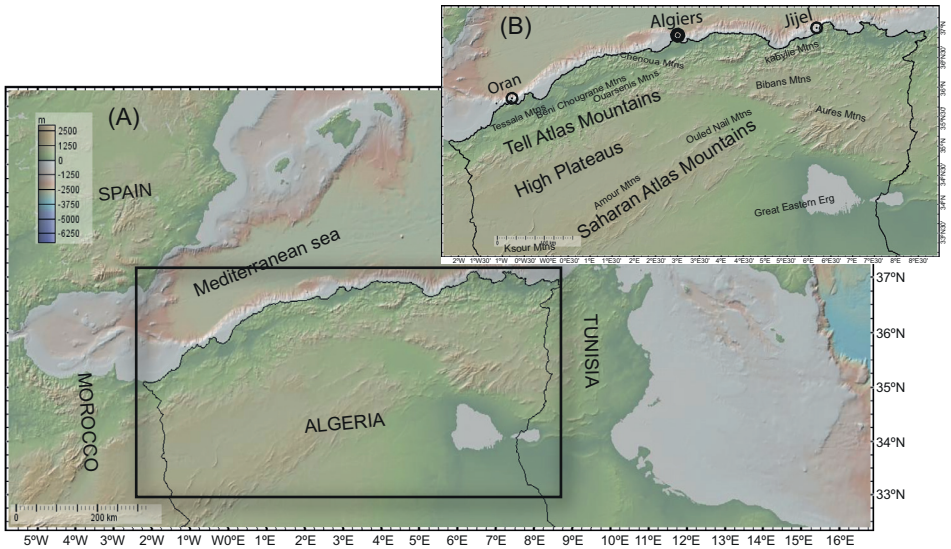

Fig. 1. (a) Topographic map of the Mediterranean Sea area, and (b) topographic map of northern Algeria showing the location of the study area. (Source: self-elaboration based on geographic data from GeoMapApp, 2024.)

and precipitation is primarily concentrated during the winter months. Rainfall levels vary significantly, ranging from 500 to over 1000 mm annually, particularly in the mountainous regions. As one moves inland, the climate gradually shifts to a semi-arid type, especially in the plains and foothills. This results in hotter summers, cooler winters, and reduced precipitation, generally less than 500 mm per year. Further south, the climate becomes arid or desert-like, characterized by persistent heat and dryness throughout the year, leading to significantly high levels of aridity.

The complex interactions between these diverse climatic conditions and topographical features contribute to the observed variability in precipitation patterns across the study area, making it an important region for examining extreme weather events.

2.1.2 Rainfall data

The rainfall data used in this study is based on daily records, which have been aggregated to calculate monthly and annual rainfall totals. The data was collected from 32 rainfall stations across northern Algeria (Fig. 2) over a 41-year period, spanning from 1982 to 2022. These stations are managed by the National Meteorological Office and the National Water Resources Agency, as detailed in Table SI in the supplementary material. Stations were selected based on the availability of consistent long observation periods, ensuring data reliability for long-term analysis.

A statistical analysis of the annual rainfall is also provided in Table SI. The dataset provides a reliable foundation for calculating extreme rainfall indices due to its homogeneous data (Kheloufi-Attou et al., 2023), enabling the identification of trends and fluctuations in the intensity of extreme rainfall events over time in the region.

2.2 Methods

This study employs a novel analytical approach that has not been previously addressed in Algeria. This approach is specifically focused on the utilization of the following: (1) the analysis of extreme rainfall intensity is conducted through the use of extreme rainfall indices; (2) the extreme value theory was employed for the evaluation of the frequency and level of extreme events through the use of the generalized extreme value (GEV) distribution model. The methodology employed utilizes these indices to determine the spatial distribution of rainfall intensity across the region. The temporal trends of each index were analyzed using the Mann-Kendall test, a

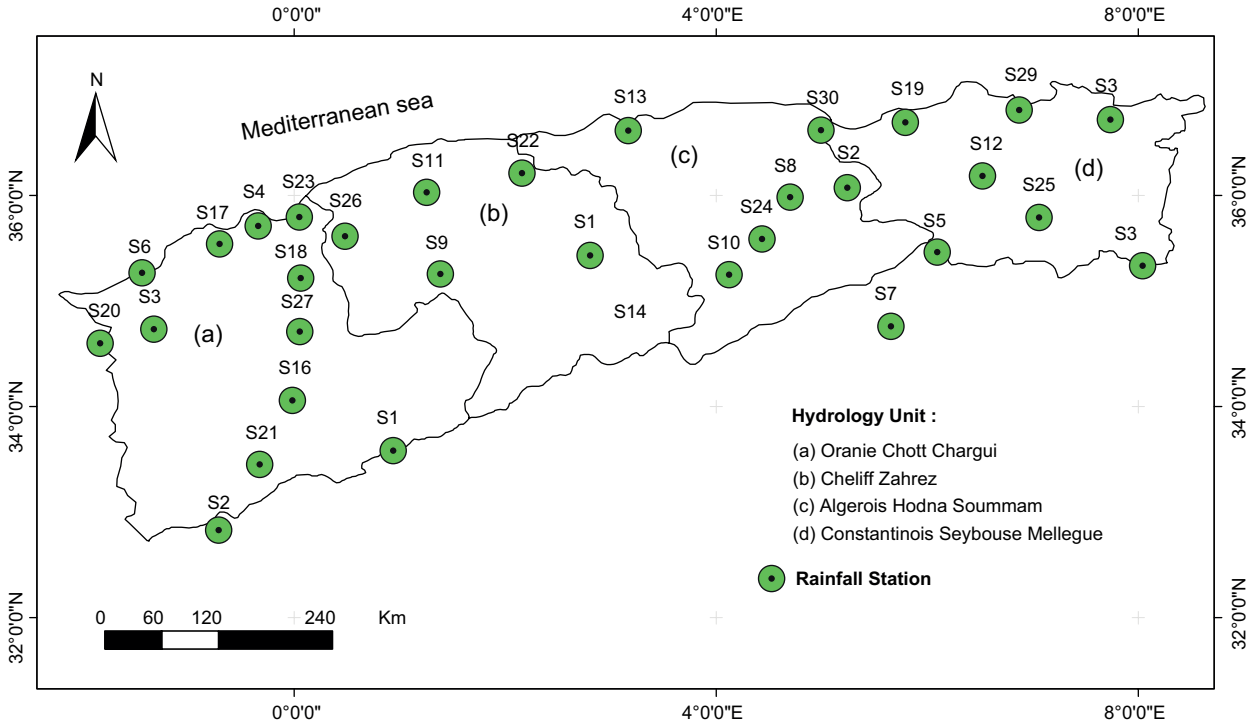

Fig. 2. Spatial distribution of rainfall stations (northern Algeria).

statistical method commonly used to identify trends in climate data. The index that exhibited the highest percentage of significant positive trends was selected for further investigation (Fig. 3).

2.2.1 Extreme rainfall indices

The method is based on six extreme precipitation indices developed by the Expert Team on Climate Change Detection and Indices to obtain a unified perspective on observed weather changes and extreme climate events (WMO, 2009). Specifically, R20mm, R95p, R99p, Rx1Day, Rx5Day, and SDII were used to monitor the intensity of extreme rainfall in northern Algeria. A user-friendly R software (RClimDex) was used for their calculation (ETCCDI, 2024). R20mm counts days with rainfall exceeding 20 mm to analyze heavy rain and flood risks. R95p and R99p track "very wet days" and "extremely rainy days" based on the 95th and 99th percentiles, respectively, aiding in flood risk and extreme weather assessment. Rx1day and Rx5day measure the highest single-day and five-day rainfall totals, highlighting risks of floods, droughts, and landslides. The simple daily intensity index (SDII) calculates the average rainfall per rainy day, monitoring changes in precipitation patterns and associated risks.

The methodology involves several stages. First, the index showing a positive trend at the majority of the examined stations is identified. Next, the quantitative relationships between the selected index and other indices are examined using Pearson correlation analysis. Following this, the trend of the identified index over the study period is analyzed. Finally, the identified index is modeled using the GEV distribution to assess the recurrence frequency and to model its spatial distribution across northern Algeria. This comprehensive approach facilitates a detailed understanding of extreme rainfall events and their implications in the region.

2.2.2 Mann-Kendall trend and moving average

According to Gilbert (1987), the Mann-Kendall test is a non-parametric method used to assess whether a variable of interest exhibits a monotonic upward or downward trend over time. This test evaluates two hypotheses: the null hypothesis (H_0), which assumes

no trend, and the alternative hypothesis (H_1), which suggests the presence of a trend. In this study, the Mann-Kendall trend test was used to detect positive or negative temporal trends in extreme rainfall indices at a 5% significance level ($\alpha = 5\%$). The test allows to determine the significance of the detected trend and quantify the percentage of trend change for each index. The index that shows a significant positive trend is further analyzed using the moving average method, applied over a five-year period, to smooth and assess the trend's progression over time.

2.2.3 Correlation

The Pearson correlation coefficient (r) (Bonett and Wright, 2000) is a widely used method for quantifying the strength and direction of the linear relationship between two variables, X and Y. This coefficient ranges from –1 to 1, where –1 signifies a perfect negative correlation, 0 indicates no correlation, and 1 denotes a perfect positive correlation. This method is particularly useful for evaluating the relationship between an index with a high trend rate and other extreme rainfall indices, providing insights into how these indices are interrelated.

$$r = \frac{\sum_{i=1}^{n}(X_i - \bar{X})(Y_i - \bar{Y})}{\sqrt{\sum_{i=1}^{n}(X_i - \bar{X})^2}\ \sqrt{\sum_{i=1}^{n}(Y_i - \bar{Y})^2}} \quad (1)$$

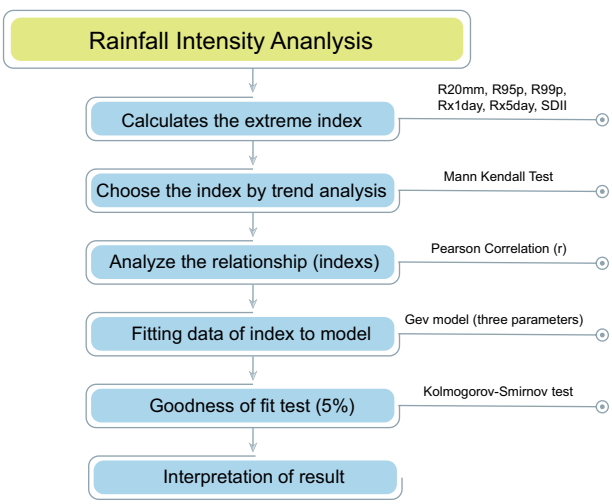

Fig. 3. Flowchart of the process for selecting and modeling the extreme rainfall index.

where $\bar{X}$ *et* $\bar{Y}$ are the means of the variables X and Y, respectively.

A critical aspect of understanding the dynamics and interconnectedness of extreme rainfall events is to analyze the Pearson correlation between rainfall intensity indices, including R20mm, R90p, R95p, R×1day, R×5day, and SDII. This analysis enables the determination of whether these indices exhibit a tendency to move in synchrony with each other.

2.2.4 Generalized extreme value (GEV) distribution

The GEV distribution, defined by Eq. (2) and characterized by three parameters—μ (location), σ (scale), and γ (shape)—is a statistical model designed to represent the extreme values in a series of observations, specifically focusing on the tail of the distribution. This approach is based on the principle of extreme values (Fisher and Tippett, 1928; von-Mises, 1936; Gnedenko, 1943; Jenkinson, 1955; Coles, 2001). The parameters of the GEV distribution are estimated using the maximum likelihood method, enabling a precise representation of the extreme events within the dataset.

$$F(x;\ \mu,\sigma,\gamma) \quad = exp \quad \left[-(1+\gamma\frac{(x-\mu)}{\sigma})^{\frac{-1}{\gamma}}\right] \quad (2)$$

The shape of the maxima in extreme-value distributions can be described by three specific distributions, depending on the value of the shape parameter γ: Gumbel, Fréchet, and Weibull. When $\gamma = 0$, the GEV distribution simplifies to the Gumbel distribution, also known as type I (Eq. 3). If γ is greater than 0, the GEV distribution corresponds to the Fréchet distribution (type II). In contrast, a negative γ leads to the Weibull distribution (type III). Each of these distributions characterizes the tail behavior of extreme values differently, offering a nuanced understanding of the underlying data.

$$F(x;\ \mu,\sigma) \quad = \exp\left[-exp\left(\frac{x-\mu}{\sigma}\right)\right] \quad (3)$$

Estimating return periods is crucial for assessing the frequency and intensity of extreme events. Eq. (4) is used to calculate the return period $F^{-1}(p)$, which corresponds to specific intervals such as five, 20, 50, and 100 years. This estimation helps to understand how often extreme events are likely to occur and their potential magnitude.

$$F^{-1}(p)=\begin{cases}\mu+\frac{\sigma}{\gamma}\left[ln(p)^{-\gamma}-1\right] & \rightarrow \quad \gamma\neq 0\\ \mu-\sigma ln\left(-ln(p)\right) & \rightarrow \quad \gamma=0\end{cases} \quad (4)$$

3. Results

3.1 Analysis of rainfall extremes

Figure 4 provides a detailed analysis of precipitation intensity across various extreme rainfall indices on an annual scale. The data covers multiple indices, revealing significant regional variations in rainfall extremes in northern Algeria.

The maximum one-day rainfall index (R×1day) shows a substantial range, from a high of 173 mm recorded in the Oran region to a low of 6 mm in the Ain-Sefra region. This considerable disparity highlights the variability in extreme one-day rainfall events across the region. The spatial distribution of mean R×1day values shows that areas such as Jijel, Soummam, Skikda, Miliana, Annaba, Dar El Beida, and Oran experience significant rainfall intensities, with mean values surpassing 50 mm. This suggests that these regions are particularly susceptible to high-intensity rainfall events, which can have considerable impacts on local infrastructure and agriculture (Fig. 4a).

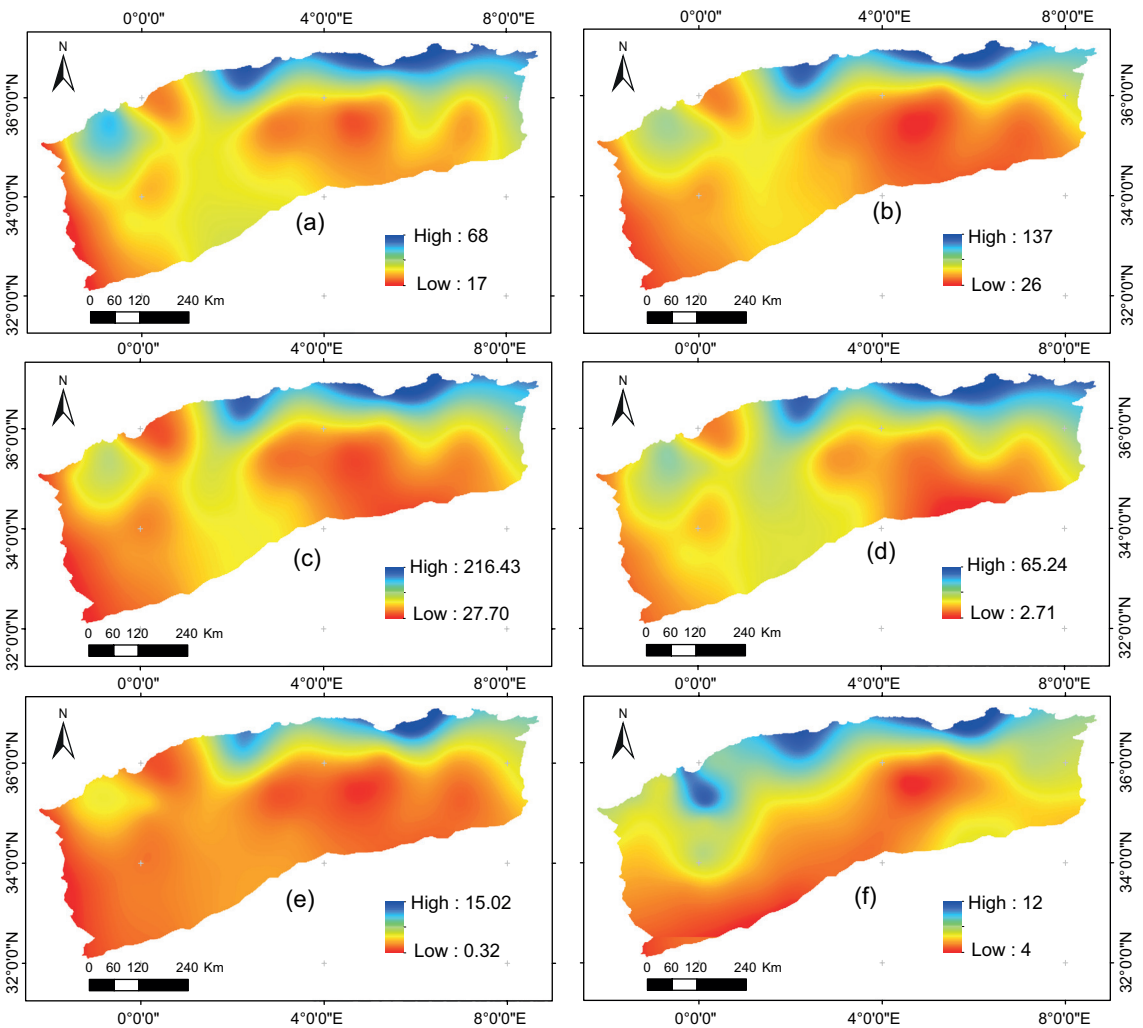

Fig. 4. Spatial distribution of extreme rainfall intensity in northern Algeria 1982-2022. (a) R×1day, (b) R×5day, (c) R95p, (d) R99p, (e) R20mm, (f) SDII.

For the maximum five-day rainfall index (R× 5day), there is notable variation, with values ranging from 300 mm in the Jijel region to just 7 mm in the Mecheria region. This variation suggests that certain areas are more prone to prolonged periods of heavy rainfall, which can result in flooding and other severe weather impacts. The analysis of mean values further reveals that Jijel, Soummam, Miliana, and Skikda experience significant rainfall, with intensities exceeding 100 mm over a five-day period. This suggests that these regions may face a higher risk of prolonged rainfall events, which could exacerbate flooding and soil erosion (Fig. 4b).

The R95p index, which measures the amount of precipitation falling on the top 5% of wettest days, reaches a maximum of 632 mm in the Soummam region. Average values for this index exceed 150 mm in Jijel, Soummam, Miliana, and Skikda, indicating that these regions frequently experience extreme rainfall events that fall into the top 5% of wettest days. This high level of extreme precipitation can significantly impact water management and flood control efforts (Fig. 4c).

Similarly, the R99p index, which represents the precipitation amount on the top 1% of wettest days, peaks at 528 mm in Soummam. Jijel, Soummam, Miliana, and Skikda also exhibit high average values, exceeding 50 mm, suggesting that these regions experience severe rainfall on the rarest, most extreme days. This underscores the potential for significant weather-related disruptions in these areas (Fig. 4d).

Regarding the number of days with precipitation exceeding 20 mm (R20mm), Jijel stands out with the highest frequency of such events, recording 26 days annually. The data indicate that Jijel, Soummam, Miliana, Skikda, and Dar El Beida experience the highest frequency of days with heavy rainfall, highlighting the vulnerability of these regions to frequent extreme rainfall events. This frequent occurrence of heavy rainfall can lead to an increased risk of flooding and challenges for flood management (Fig. 4e).

Finally, the SDII, which measures the intensity of precipitation on wet days, shows relatively low values in Jijel, Miliana, Ghriss, Soummam, and Arzew, with values of 11.64, 9.88, 9.85, 9.58, and 9.50, respectively. Lower SDII values indicate that, while these regions experience high-intensity rainfall events, the average daily rainfall during wet days may be less extreme compared to other regions. This provides a nuanced view of rainfall intensity, emphasizing that even regions with low SDII can still experience significant rainfall impacts (Fig. 4f).

Overall, this comprehensive analysis highlights the significant variability in extreme rainfall events across northern Algeria, with a particular focus on regions most affected by high-intensity and frequent rainfall. Understanding these patterns is crucial for effective water resource management, flood control, and climate adaptation strategies.

3.2 Analysis of the Mann-Kendall trend

The trend analysis of extreme precipitation indices provides deeper insights into the variability and changes in extreme rainfall events across northern Algeria (Fig. 5). This analysis complements the previous examination of rainfall extremes and highlights significant patterns and discrepancies.

The maximum one-day rainfall index (R×1day) shows a mixed trend across the region. A positive trend is observed at 13 stations, indicating that these locations experience increasingly intense one-day rainfall events over time. Conversely, 11 stations exhibit a negative trend, suggesting a reduction in the magnitude of extreme one-day rainfall events in these areas. This variability reflects the heterogeneous nature of extreme one-day rainfall across northern Algeria, with some areas experiencing intensified extremes while others see a decrease. This trend aligns with the earlier finding that the Oran region had the highest maximum one-day rainfall (173 mm), while other regions, such as Ain-Sefra, recorded much lower values (6 mm), illustrating the spatial variability in extreme rainfall.

For the maximum five-day rainfall index (R ×5day), the analysis reveals a positive trend at 18 stations and a negative trend at 10 stations. This indicates that most regions are experiencing increased intensity of extreme rainfall over extended periods, with notable variability. This finding corresponds to the earlier observation where Jijel and Mecheria exhibited significant variation in five-day rainfall, with Jijel recording higher values (300 mm) compared to Mecheria (7 mm). The positive trend at most stations suggests that prolonged heavy rainfall events are becoming more common in many areas.

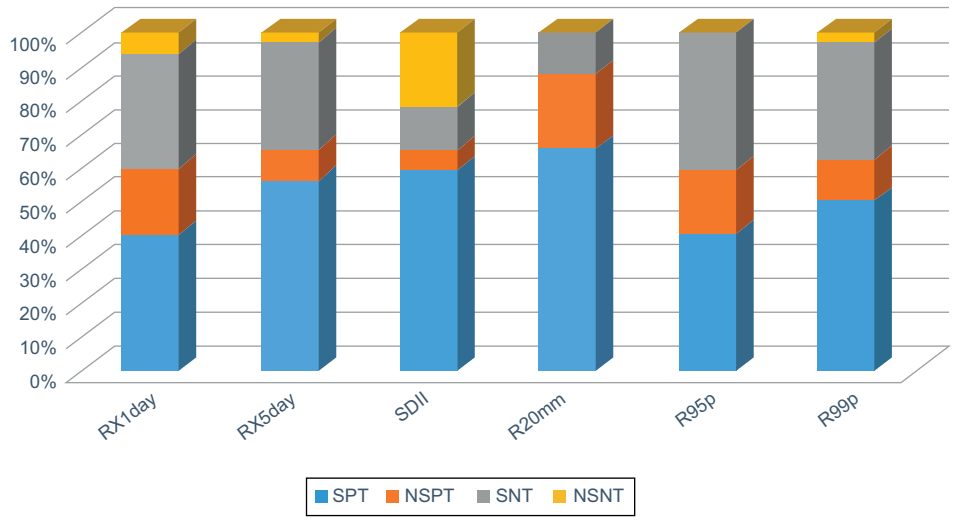

Fig. 5. Percentage of stations for each extreme precipitation index, a significant positive trend (SPT), a non-significant positive trend (NSPT), a significant negative trend (SNT), and a non-significant negative trend (NSNT).

The SDII displays a predominantly positive trend at 19 stations and a negative trend at four stations. This indicates an overall increase in rainfall intensity during wet days, aligning with the observation that regions like Jijel and Soummam experience high rainfall intensity. The notable increase in SDII values complements the earlier findings where Jijel had the highest frequency of days with rainfall exceeding 20 mm.

The number of days with rainfall exceeding 20 mm (R20mm) shows a significant positive trend at 21 meteorological stations, with only four stations indicating a negative trend. This widespread positive trajectory reflects the earlier observation that Jijel experienced the highest number of days with rainfall over 20 mm. The increase in R20mm values aligns with the observation of frequent extreme rainfall days in the northeastern region of Algeria.

The R95p index, representing precipitation on the top 5% of wettest days, shows an unequal number of stations with positive and negative trends, with 13 stations exhibiting negative trends. This suggests a variability in extreme precipitation events across the region, with the positive trend concentrated in the western region. In contrast, the R99p index exhibits a positive trend at 16 stations and a negative trend at 11 stations, suggesting a general increase in the intensity of the rarest extreme rainfall events. This finding complements the observation that Soummam had the highest R99p values (528 mm), highlighting regions experiencing more severe extreme rainfall.

The trend analysis of extreme precipitation indices, when compared to previously observed extreme rainfall patterns, offers several important insights. Firstly, there is significant regional variability in extreme precipitation across northern Algeria. This variability reflects the diverse spatial patterns observed earlier, with regions such as Jijel and Soummam consistently showing high values across various indices while other areas display more mixed trends. Secondly, there is a general trend toward increasing intensity in indices such as Rx5day, SDII, R20mm, and R99p. This trend aligns with earlier findings of significant extreme rainfall events (Bessaklia et al., 2018), particularly in areas such as Jijel and Soummam, suggesting that these regions are experiencing an escalation in extreme weather events. Thirdly, the increase in the number of days with high rainfall (R20mm) and the higher intensity values (SDII) observed earlier are supported by the positive trends in these indices, emphasizing the growing frequency and intensity of extreme rainfall. Lastly, the contrasting trends observed in the R95p and R99p indices offer insight into the varying experiences of extreme precipitation across the study area. While some regions have witnessed an increase in extreme precipitation, others have demonstrated stability or

even a decline in this phenomenon. This reflects the complex interplay of climatic factors affecting the region. Overall, the trend analysis highlights the dynamic nature of extreme precipitation in northern Algeria, with significant regional variations and a general trend toward more intense extreme rainfall events.

3.3 Relationship between R20mm and other indices

The Pearson correlation coefficient reveals significant relationships between the R20mm index, which measures the number of days with rainfall exceeding 20 mm, and other indices of extreme precipitation. The correlation between the R20mm and R95p indices (Fig. 6a) ranges from 0.965 to 0.447, indicating a notably strong positive correlation in several regions. Specifically, regions such as El Bayadh, Bou Chekif, Batna, Bordj Bou Arreridj, Djelfa, Oum El Bouaghi, Setif (Ain Arnat), Mecheria, Ain Sefra, Saida, and Biskra exhibit a Pearson correlation coefficient exceeding 0.900, suggesting that these areas experience a strong relationship between the frequency of heavy rainfall days and the volume of extreme precipitation falling on the wettest days.

The correlation between the R20mm and R99p indices (Fig. 6b) ranges from 0.901 to –0.136, demonstrating considerable variability across different

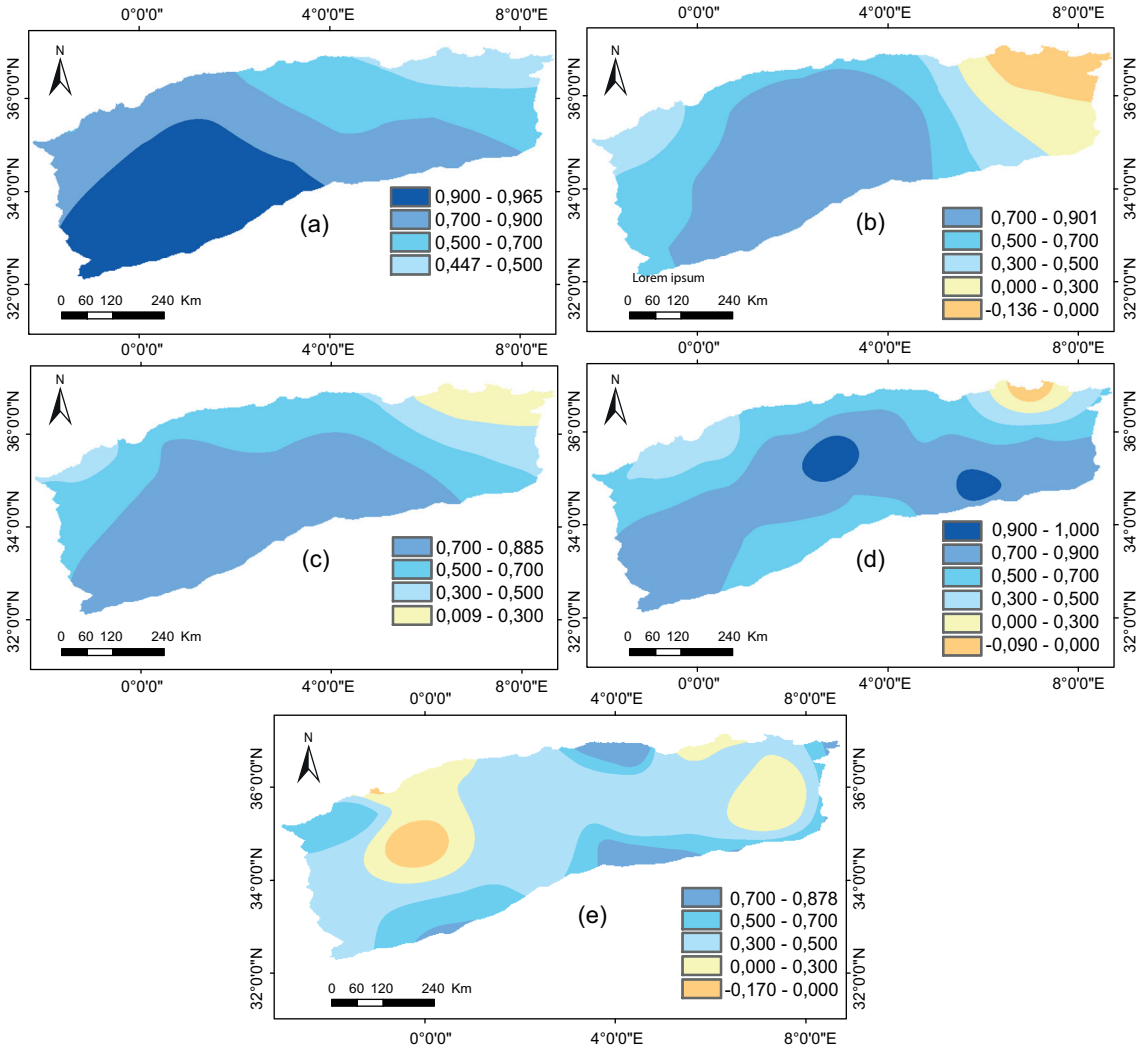

Fig. 6. Correlation coefficient between the R20mm index and the (a) R95p, (b) R99p, (c) R×1day, (d) R×-5day, and (e) SDII indices.

regions. In the regions such as S1, S9, S10, S16, S20, and S24, the correlation coefficient exceeds 0.700, indicating a robust positive relationship. This implies that in these areas, an increase in the number of days with heavy rainfall is closely associated with more intense precipitation on the top 1% of wettest days, highlighting the vulnerability of these regions to extreme weather events.

Similarly, the correlation between the R20mm and R×1day indices (Fig. 6c) ranges from 0.885 to 0.009. Regions such as S2, S7, S10, S16, S20, S23, S24, S25, and S26 exhibit a pronounced correlation, with coefficients exceeding 0.700, which suggests that in these regions, the number of days with heavy rainfall is strongly linked to the maximum one-day rainfall amount, emphasizing the impact of single-day extreme events on local precipitation patterns.

The relationship between R20mm and R×5day indices (Fig. 6d), with a correlation ranging from 1.000 to –0.090, further highlights the variability in regional precipitation dynamics. Regions such as S1, S2, S7, S9, S10, S16, and S31 exhibit a strong correlation above 0.700, indicating that these areas are prone to experiencing both frequent heavy rainfall days and significant five-day cumulative rainfall events.

Finally, the correlation between the R20mm and the SDII indices (Fig. 6e), which measures the average intensity of rainfall on wet days, spans from 0.878 to –0.170. Regions including S2, S3, S7, S13, S15, S30, and S32 exhibit a strong positive correlation, with coefficients exceeding 0.700. This suggests that in these regions, an increase in the number of days with heavy rainfall is closely linked to a higher average rainfall intensity on those days.

Overall, the analysis of these correlations highlights the complex and region-specific relationships between various extreme precipitation indices in northern Algeria. The strong positive correlations in several regions suggest that these areas are particularly vulnerable to extreme rainfall events, with significant impacts on local hydrology, agriculture, and infrastructure.

3.4 Historical analysis of the R20mm index fluctuations

Fluctuations in cumulative daily precipitation exceeding or equal to 20 mm are evaluated using the five-year moving average method, as shown in Figure 7. This method is instrumental in revealing temporal changes in extreme precipitation conditions, specifically through the lens of the R20mm index. Over time, significant accumulations of precipitation above 20 mm have been recorded in various regions across northern Algeria, highlighting distinct temporal and spatial patterns.

In the western region, a marked increase in extreme precipitation was observed between 2000 and 2010. Stations such as Maghnia (Fig. 7a), Ain Sefra (Fig. 7b), and Saida (Fig. 7c) recorded substantial rises in cumulative precipitation during this period. Additionally, similar trends were noted in the areas surrounding the Arzew, Beni Saf, and El Kheiter stations. This surge in precipitation frequency and intensity in the western region suggests an increasing vulnerability to extreme weather events during the early 21st century.

The central part of the study area also exhibited a significant increase in extreme precipitation events. This resulted in a heightened frequency of rainfall exceeding 20 mm, particularly pronounced in the Miliana region (Fig. 7d). In this area, the moving average highlights a distinct rise in extreme rainfall events during the 2000s. This trend, however, is followed by a subsequent decline in the 2010s, as observed in the Bou Saâda region (Fig. 7f). This fluctuation suggests a complex interaction of climatic factors contributing to both the rise and fall of extreme precipitation events in this central region.

In the eastern region, the R20mm index shows a significant upward trend from the 2000s onward, with stations such as Setif (Ain Arnat), Jijel, Tébessa, and Oum El Bouaghi (Fig. 7i) being particularly affected. These areas experienced a notable increase in the frequency and intensity of extreme rainfall events, indicating a shift towards more volatile and extreme precipitation patterns in the eastern part of northern Algeria.

This analysis underscores the dynamic and region-specific nature of extreme precipitation in northern Algeria. The western, central, and eastern regions each exhibit distinct temporal patterns in extreme rainfall, reflecting the complex climatic influences across the region. The observed increases in the R20mm index during specific periods suggest an overall trend towards more frequent and intense extreme weather events, although these trends are not

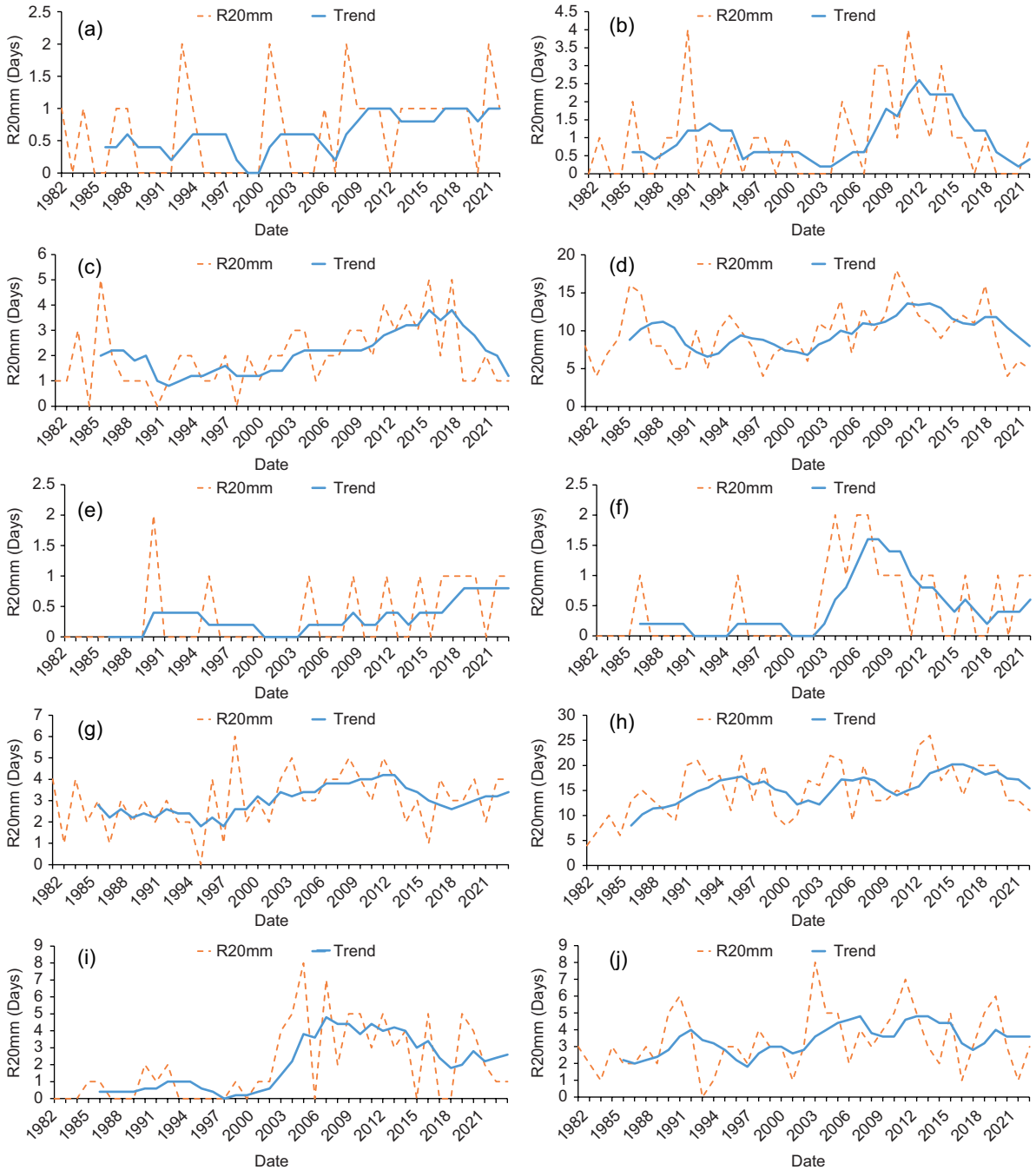

Fig. 7. Temporal trend of the R20mm index from 1982 to 2022 in the stations: (a) Maghnia, (b) Ain Sefra, (c) Saida, (d) Miliana, (e) M'Sila, (f) Bou Saada, (g) Setif(Ain Arnat), (h) Jijel, (i) Oum El Bouaghi, (j) Tebessa.

uniformly distributed across all regions. The moving average method, as illustrated in Figure 7, provides a clearer understanding of these temporal changes, highlighting the need for regionally tailored strategies to mitigate the impacts of extreme precipitation and to adapt to evolving climatic conditions.

3.5 Analyzes of extreme values

3.5.1 Fitting the generalized extreme value (GEV) distribution

The analysis of extreme values was conducted using the GEV distribution to fit precipitation events exceeding 20 mm. This approach enables the estimation of the distribution's shape, scale, and location parameters, providing insights into the behavior of extreme precipitation across various regions in northern Algeria. The shape parameter (γ) varies across stations, with values ranging from 0.579 to –0.113. This variation indicates that most of the R20mm index series align with the Fréchet distribution (type II), characterized by heavy tails, suggesting a higher likelihood of extreme rainfall events. The exception to this trend is the S10 station, located in the central region of the study area, where the shape coefficient is negative ($\gamma = -0.113$), indicating a Weibull distribution (type III), characterized by lighter tails and a lower probability of extreme values.

The scale parameter (σ), which indicates the spread of the distribution, ranges from 8.967 to 0.366. A higher scale parameter suggests greater variability in extreme rainfall events, with some regions experiencing more significant fluctuations in the magnitude of extreme precipitation. The location parameter (μ), representing the central tendency of the distribution, falls between 27.468 and 21.439. This parameter provides an estimate of the central value around which extreme events cluster, with higher values indicating regions more prone to intense rainfall events.

3.5.2 Goodness-of-fit tests

Table I presents the results of the goodness-of-fit tests for the GEV distribution applied to the R20mm index. The Kolmogorov-Smirnov test was used to assess the fit, with the null hypothesis (H_0) positing that the observed data follows the GEV distribution. The null hypothesis for 26 precipitation stations was accepted at the significance level of $\alpha = 5\%$. The fit was verified for six stations, although at the stricter $\alpha = 1\%$ significance level: S19, S22, S28, S29, S30, and S31. However, at station S3, the null hypothesis was disproved. This indicates that, although the GEV distribution is a suitable model for overall harsh precipitation in northern Algeria, the fit is stronger in some areas, particularly those with more frequent or severe extreme events.

The analysis of extreme values highlights the spatial variability in the behavior of extreme precipitation across northern Algeria. Regions exhibiting positive shape parameters and a good fit with the Fréchet distribution are more likely to experience severe and frequent extreme rainfall events. In contrast, areas with a negative shape parameter, like Bou Saâda, are less prone to such extremes. The differences in scale and location parameters further highlight the diversity of precipitation patterns across the region, with some areas experiencing higher variability and others exhibiting a more stable pattern of extreme events.

These findings underscore the importance of region-specific analyses when assessing the risk of extreme weather events. The use of the GEV distribution provides a robust framework for understanding and predicting extreme precipitation, which is crucial for developing effective mitigation and adaptation strategies in the face of changing climate conditions. The observed variations across different stations also suggest that local geographic and climatic factors play a significant role in shaping the distribution and intensity of extreme rainfall events in northern Algeria.

3.5.3 Recurrence frequency of extreme rainfall

The recurrence frequency of extreme precipitation events, specifically those exceeding 20 mm, has been analyzed using the GEV distribution. This analysis offers insights into the likely frequency of such events across different return periods, specifically five, 20, 50, and 100 years, in various regions of northern Algeria.

The R20mm index, which measures the number of days with daily precipitation above 20 mm, shows a range of expected values across the specified return periods. For a five-year return period, the index ranges between 25 and 42 mm. During this period, the regions around the Soummam, Jijel, Skikda, Miliana, Dar El Beida, and Biskra stations are observed to experience rainfall amounts ranging from 42 to 35 mm. On the other hand, the western regions of the study area record lower rainfall levels, generally below 30 mm, within the same return period (Fig. 8a).

When examining a 20-year return period, the R20mm index ranges from 27 to 63 mm. The analysis reveals that regions such as Soummam, Jijel, Miliana,

Table I. Parameters distribution and Kolmogorov-Smirnov test.

Station	Parameters			Kolmogorov-Smirnov test	
	γ	σ	μ	S value	p value
S1	0.219	2.472	22.331	0.121	0.670
S2	0.263	3.446	22.667	0.136	0.447
S3	0.366	0.366	24.727	0.112	**0.002**
S4	0.405	3.838	23.109	0.077	0.684
S5	0.301	4.907	23.765	0.101	0.317
S6	0.399	4.693	23.889	0.095	0.155
S7	0.084	8.966	27.468	0.157	0.152
S8	0.239	4.357	23.605	0.101	0.190
S9	0.280	4.845	23.776	0.089	0.322
S10	-0.113	5.459	25.378	0.085	0.997
S11	0.313	5.232	24.181	0.101	0.120
S12	0.391	5.195	24.246	0.084	0.152
S13	0.290	6.269	25.369	0.073	0.086
S14	0.223	3.732	23.662	0.103	0.393
S15	0.241	5.452	24.754	0.074	0.768
S16	0.388	3.389	23.189	0.084	0.840
S17	0.192	6.657	25.502	0.104	0.090
S18	0.531	3.484	22.973	0.052	0.842
S19	0.267	7.242	26.421	0.065	**0.011**
S20	0.579	2.006	21.439	0.094	0.958
S21	0.299	5.875	25.000	0.138	0.197
S22	0.286	6.884	25.856	0.071	**0.039**
S23	0.402	2.475	22.311	0.097	0.912
S24	0.243	2.802	22.653	0.142	0.925
S25	0.304	4.438	23.613	0.084	0.598
S26	0.092	4.083	23.831	0.087	0.987
S27	0.332	4.546	24.032	0.082	0.612
S28	0.176	4.835	23.711	0.143	**0.011**
S29	0.373	5.803	24.731	0.082	**0.017**
S30	0.321	7.368	26.392	0.069	**0.040**
S31	0.238	5.501	24.347	0.126	**0.026**
S32	0.337	4.954	24.599	0.088	0.328

Figures in bold indicate that the null hypothesis H_0 has been accepted at a significance level of $\alpha = 1\%$.

Biskra, Skikda, Dar El Beida, Constantine, Mecheria, Es Senia, and Beni Saf are likely to experience extreme rainfall events, ranging from 63 to 50 mm. In contrast, regions such as Mostaganem, M'Sila, Ain Oussara, and Annaba exhibit lower levels of extreme rainfall, with values ranging from 37 to 26 mm (Fig. 8b).

The trend continues over a 50-year return period, where the R20mm index expands to a range of 28 to 84 mm. In this period, extreme rainfall episodes of between 84 and 67 mm are anticipated in the Soummam, Jijel, Skikda, Miliana, Constantine, Dar El Beida, Biskra, Ghriss, Mecheria, and Beni Saf regions. Conversely, the Ain Oussara and Annaba regions are expected to experience significantly lower rainfall, with values below 38 mm (Fig. 8c).

For the 100-year return period, the R20mm index ranges from 29 to 104 mm. The regions most affected by extreme rainfall, with levels ranging from 85 to 104 mm, include Soummam, Skikda, Ghriss, Jijel, Miliana, Constantine, Beni Saf, and Dar El Beida. Meanwhile, regions such as Bou Saâda, Ain Oussara,

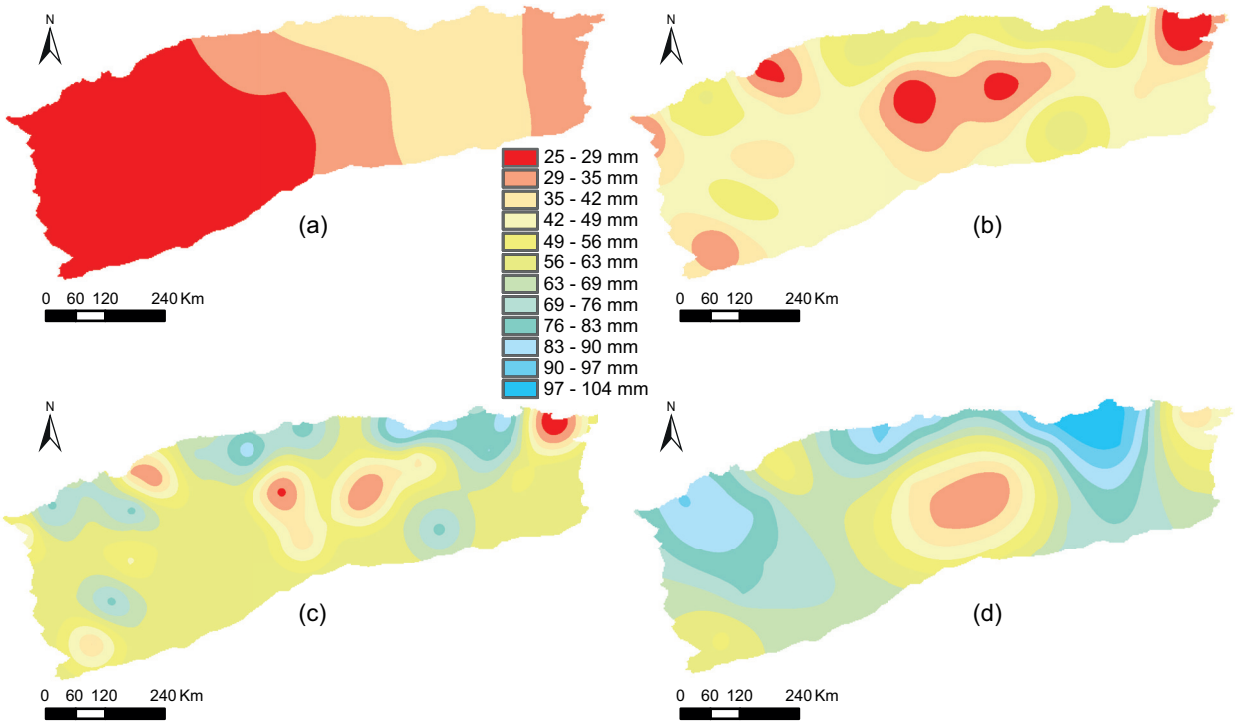

Fig. 8. Spatial distribution of R20mm return periods: (a) five years, (b) 20 years, (c) 50 years, (d) 100 years.

and Annaba are characterized by notably lower rainfall levels, generally below 45 mm (Fig. 8d).

This analysis highlights significant regional disparities in the recurrence of extreme rainfall events. Coastal and mountainous areas, particularly in the eastern and central parts of northern Algeria, are more prone to high-intensity rainfall events in all return periods. These regions, which include Soummam, Jijel, Skikda, and Miliana, are among those that consistently experience the highest levels of extreme rainfall. In contrast, the western and southern regions, as well as some areas of the central high plains, including Bou Saada, Ain Oussera, and the Annaba region, located to the east of the study area, are less affected, with significantly lower expected rainfall intensities.

The observed patterns suggest that the eastern and central regions of northern Algeria are more vulnerable to extreme weather events, which could have significant implications for water resource management, infrastructure planning, and disaster preparedness in these areas.

4. Discussion

The primary goal of this study is to investigate the spatiotemporal variability of extreme rainfall indices across northern Algeria by modeling an index that demonstrates the trends at the majority of the stations examined. This was achieved using the non-parametric Mann-Kendall test and the GEV distribution. To assess rainfall intensity, the study utilized indices such as R×1Day, R×5Day, R95p, R99p, R20mm, and SDII. Prior research has explored extreme rainfall indices at various spatial resolutions across different regions, continents, and even globally (Nastos et al., 2013; Alexander et al., 2019; Ndiaye et al., 2023; Hamitouche et al., 2024a; El-Hawari et al., 2024). This context allows for a comparative analysis of the values obtained in regions with varying climatic conditions.

The results reveal that rainfall intensity in northern Algeria has evolved, with the majority of extreme precipitation events concentrated in the coastal regions, especially in the eastern part of the study area. These findings are in accordance with the results of

the study conducted by Bessaklia et al. (2021) in eastern Algeria, which revealed an increasing concentration of extreme rainfall indices in the coastal zone and in the high-altitude regions, and also revealed that the intensity of rainfall exhibits a decline in southerly directions. The analysis indicates that 19, 38, 35, 38, 34, and 44% of the stations show above-average values for the R20mm, R95p, R99p, R×1day, R×5day, and SDII indices, respectively.

The Mann-Kendall test further identifies both positive and negative trends across these indices, accounting for the significance levels of the null hypothesis (H_0). The R×1day index shows a rate of 41%, the R×5day rate is 56%, the SDII index has a notable rate of 59%, and the R20mm index shows a rate of 66%. Meanwhile, the R95p index reaches 41%, and the R99p index stands out with a rate of 50%. These findings align with those of Benaïchata et al. (2015), who used extreme rainfall indices to detect climate change in Algeria. The ratios for the R×5day, SDII, and R20mm indices being over 50% suggest that most stations are recording an increase in rainfall intensity of more than 20 mm over a five-day period. The R20mm index shows an increase in precipitation frequency at over 88% of the surveyed stations, highlighting the index's distinct pattern compared to others. This observation is consistent with studies by Filahi et al. (2016) on extreme rainfall trends in Morocco and Camarasa-Belmonte et al. (2020), who noted a positive trend in rainfall intensity in the eastern part of Spain from 1989 to 2016. Hamitouche et al. (2024b) also reported similar trends.

A Pearson correlation analysis between the R20mm index and other extreme rainfall indices reveals a strong correlation between the R20mm index and R95p, indicating that daily precipitation events exceeding 20 mm have a direct influence on the R95p index. Temporal analysis using the moving average method shows a significant upward trend in R20mm at most stations from the 2000s onward, confirming that rainfall episodes exceeding 20 mm contribute to an increase in rainfall intensity in northern Algeria.

To define extreme precipitation events, the GEV distribution was applied to episodes of precipitation equal to or greater than 20 mm. The GEV model parameters reveal that 99% of the stations exhibit positive shape parameters consistent with the Fréchet distribution, indicating a higher likelihood of extreme R20mm values occurring. This finding supports the conclusions of Boudrissa et al. (2017), who also found the Fréchet distribution to be appropriate for extreme events, given its higher suitability for rare occurrences compared to the Gumbel and Weibull distributions. The location parameter (μ) across stations exceeds the average precipitation of ≥ 20 mm, with a maximum difference of 8 mm, indicating that extreme precipitation events generally exceed the 20 mm average threshold. Additionally, the scale parameter (σ) is observed to exceed 6 mm at several stations, including Biskra, Soummam, Jijel, Miliana, Es Senia, and Dar El Beida, indicating that extreme precipitation events can vary by approximately $\pm$ 6 mm from the annual average. The Kolmogorov-Smirnov test further indicates that the null hypothesis (H_0) is accepted at 78 and 22% of stations for the $\alpha = 5\%$ and the $\alpha = 1\%$ significance levels, respectively, confirming the applicability of the GEV model to R20mm data. This is consistent with findings by Benaini et al. (2023), who validated the GEV model for data from 180 stations across northeastern Algeria using the Kolmogorov-Smirnov test.

The validated models enable the assessment of extreme rainfall frequency. The majority of precipitation occurs in the central part of the study area, with maximum values ranging from 35 to 42 mm during the five-year return period. The western region, however, exhibits the lowest precipitation levels, ranging from 25 to 29 mm. In contrast, during the 20-, 50-, and 100-year return periods, the scenario shifts, with minimum values observed in the central zone (Ain Oussara, Bou Saâda, M'Sila, and Bordj Bou Arreridj) and Mostaganem (west) and Annaba (east), with precipitation levels ranging from 25 to 35 mm. Extreme rainfall is widespread across the study area, with intervals ranging from 63 to 104 mm, except in the central zone, Mostaganem, and Annaba regions.

While localized variations in extreme precipitation are expected, the implications for Algeria are significant, particularly for socioeconomic and climate-sensitive sectors, such as water resources and agriculture. The intense precipitation observed could jeopardize the recharge capacity of aquifers and other water storage structures in the medium to long term due to the increased runoff rates and reduced soil infiltration capacity. In conclusion, this study reveals a notable increase in the frequency of extreme precipitation events

linked to daily rainfall ≥ 20 mm, highlighting the growing significance of such extreme weather events in the study region. This underscores the necessity of continuous monitoring and heightened awareness of extreme weather patterns, particularly in the context of climate change. Such understanding is crucial for the development of effective adaptation policies and strategies that aim to mitigate the adverse impacts on communities and ecosystems.

5. Conclusion

This study provides a comprehensive analysis of the spatiotemporal variability of extreme rainfall events in northern Algeria, focusing on indices such as R×1Day, R×5Day, R95p, R99p, R20mm, and SDII. These approaches provide a comprehensive examination of extreme precipitation occurrences and their spatial distribution within the region. The findings reveal a notable increase in the frequency and intensity of extreme precipitation events, particularly in coastal and high-altitude regions, with the R20mm index showing the most significant upward trend. These trends align with previous studies, indicating that extreme rainfall is becoming increasingly concentrated in specific areas, particularly in the eastern and coastal zones. The application of the generalized extreme value (GEV) distribution further supports these findings, suggesting that extreme precipitation events exceeding 20 mm are becoming more frequent.

The analysis of rainfall patterns and return periods highlights the potential hydrological impacts, particularly the increased risk of flooding, reduced soil infiltration, and challenges to water resource management in northern Algeria. This underscores the necessity for continuous monitoring and adaptive strategies to address the growing risk of extreme weather events, which are expected to have significant socioeconomic implications, particularly for agriculture and water resources.

The analysis was based on modeled data spanning 41 years (1982-2022). It is recommended to extend the study period to enhance the detection of extremely rare events. On the contrary, the application of the GEV model significantly contributed to highlighting the frequency and understanding of the variability of extreme precipitation, as well as its spatial distribution, during the associated return periods. These results indicate that northern Algeria is exposed to significant return levels exceeding 100 mm, particularly in coastal regions and the south, associated with the 100-year return period. Therefore, the results obtained can be used for risk assessment in the study area, as well as for comparisons with simulations from regional and global models. For example, this can be used to assess the impact of regional and continental climate change on extreme rainfall in northern Algeria by developing projections of the magnitude of future events.

References

Alexander LV, Fowler HJ, Bador M, Behrangi A, Donat MG, Dunn R, Funk C, Goldie J, Lewis E, Rogé M, Seneviratne SI, Venugopal V. 2019. On the use of indices to study extreme precipitation on sub-daily and daily timescales. Environmental Research Letters 14: 125008. https://doi.org/10.1088/1748-9326/ab51b6

Asadieh B, Krakauer NY. 2015. Global trends in extreme precipitation: Climate models versus observations. Hydrology and Earth System Sciences 19: 877-891. https://doi.org/10.5194/hess-19-877-2015

Azioune R, Benhamrouche A, Tatar H, Martín-Vide J, Pham QB. 2023. Analysis of daily rainfall concentration in northeastern Algeria 1980-2012. Theoretical and Applied Climatology 153: 1361-1370. https://doi.org/10.1007/s00704-023-04526-w

Benaïchata L, Mederbal K, Chouieb M. 2015. Climate change detection with extreme weather factors concerning Algeria. European Scientific Journal 11: 220-232.

Benaini M, Achite M, Amin MGM, Singh VP. 2023. Frequency analysis of annual maximum daily precipitation in northeastern Algeria: Mapping and implications under climate variability. Theoretical and Applied Climatology 153: 1411-1424. https://doi.org/10.1007/s00704-023-04525-x

Bendjema L, Baba-Hamed K, Bouanani A. 2019. Characterization of the climatic drought indices application to the Mellah catchment, North-East of Algeria. Journal of Water and Land Development 43: 28-40. https://doi.org/10.2478/jwld-2019-0060

Bessaklia H, Ghenim AN, Megnounif A, Martín-Vide J. 2018. Spatial variability of concentration and aggressiveness of precipitation in North-East of Algeria. Journal of Water and Land Development 36: 3-15. https://doi.org/10.2478/jwld-2018-0001

Bessaklia H, Serrano-Notivoli R, Ghenim AN, Chikh HA, Megnounif A. 2021. Extreme precipitation trends in northeast Algeria using a high-resolution gridded daily dataset. International Journal of Climatology 41: 6573-6588. https://doi.org/10.1002/joc.7213

Bonett DG, Wright TA. 2000. Sample size requirements for estimating Pearson, Kendall, and Spearman correlations. Psychometrika 65: 23-28. https://doi.org/10.1007/BF02294183

Boudrissa N, Cheraitia H, Halimi L. 2017. Modelling maximum daily yearly rainfall in northern Algeria using generalized extreme value distributions from 1936 to 2009. Meteorological Applications 24: 114-119. https://doi.org/10.1002/met.1610

Camarasa-Belmonte AM, Rubio M, Salas J. 2020. Rainfall events and climate change in Mediterranean environments: An alarming shift from resource to risk in Eastern Spain. Natural Hazards 103: 423-445. https://doi.org/10.1007/s11069-020-03994-x

Clarke B, Otto F, Stuart-Smith R, Harrington L. 2022. Extreme weather impacts of climate change: An attribution perspective. Environmental Research: Climate 1: 012001. https://doi.org/10.1088/2752-5295/ac6e7d

Coles S. 2001. An introduction to statistical modeling of extreme values. Springer, London, 223 pp.

Easterling DR, Meehl GA, Parmesan C, Changnon SA, Karl TR, Mearns LO. 2000. Climate extremes: Observations, modeling, and impacts. Science 289: 2068-2074. https://doi.org/10.1126/science.289.5487.2068

El Hawari J, Yazami Ztait M, Bouhafa Y, El Ghachi M. 2024. Evolution of extreme climatic phenomena in the Central-West of Morocco: Case of the city of Agadir. Revue Internationale de la Recherche Scientifique 2: 589-601. https://doi.org/10.5281/zenodo.10993523

ETCCDI. 2024. Expert Team on Climate Change Detection and Indices. Available at: https://etccdi.pacificclimate.org/software.shtml (accessed 19 May 2024).

Filahi S, Tanarhte M, Mouhir L, El-Morhit M, Tramblay Y. 2016. Trends in indices of daily temperature and precipitations extremes in Morocco. Theoretical and Applied Climatology 124: 959-972. https://doi.org/10.1007/s00704-015-1472-4

Fisher RA, Tippett LHC. 1928. Limiting forms of the frequency distribution of the largest or smallest member of a sample. Mathematical Proceedings of the Cambridge Philosophical Society 24: 180-190. https://doi.org/10.1017/S0305004100015681

GeoMapApp. 2024. GeoMapApp v. 3.7.4. A map-based application for browsing, visualizing, and analyzing global and regional geoscience data sets, including geophysics, geology, geochemistry, and climatology. Available at: http://www.geomapapp.org/ (accessed 02 July 2024).

Ghenim AN, Megnounif A, Seddini A, Terfous A. 2010. Fluctuations hydropluviométriques du bassin-versant de l'oued Tafna à Béni Bahdel (Nord-Ouest algérien). Science et Changements Planétaires: Sécheresse 21: 115-120. https://doi.org/10.1684/sec.2010.0240

Ghenim AN, Megnounif A. 2016. Variability and trend of annual maximum daily rainfall in northern Algeria. International Journal of Geophysics 2016: 6820397. https://doi.org/10.1155/2016/6820397

Gilbert RO. 1987. Statistical methods for environmental pollution monitoring. Van Nostrand Reinhold, New York, 336 pp.

Giorgi F, Lionello P. 2008. Climate change projections for the Mediterranean region. Global and Planetary Change 63: 90-104. https://doi.org/10.1016/j.gloplacha.2007.09.005

Gnedenko B. 1943. Sur la distribution limite du terme maximum d'une série aléatoire. Annals of Mathematics 44: 423-453. https://doi.org/10.2307/1968974

Hamitouche Y, Zeroual A, Meddi M, Assani AA, Alkama R. 2024a. Changes in extreme precipitation indices across Algeria climate zones. International Journal of Climatology 44: 2537-2560. https://doi.org/10.1002/joc.8467

Hamitouche Y, Zeroual A, Meddi M, Assani AA, Alkama R, Şen Z, Zhang X. 2024b. Projected changes in extreme precipitation patterns across Algerian sub-regions. Water 16: 1353. https://doi.org/10.3390/w16101353

IPCC. 2021. Climate change 2021: The physical science basis. Working Group I contribution to the Sixth Assessment Report of the Intergovernmental Panel on Climate Change (Masson-Delmotte V, Zhai P, Pirani A, Connors SL, Péan C, Berger S, Caud N, Chen Y, Goldfarb L, Gomis MI, Huang M, Leitzell K, Lonnoy E, Matthews JBR, Maycok TK, Waterfield T, Yelekçi O, Yu R, Zhou B, Eds.). Cambridge University Press, Cambridge, USA, 2391 pp. https://doi.org/10.1017/9781009157896

Jenkinson AF. 1955. The frequency distribution of the annual maximum (or minimum) values of meteorological elements. Quarterly Journal of the Royal Meteorological Society 81: 158-171. https://doi.org/10.1002/qj.49708134804

Jiménez-Esteve B, Barriopedro D, Johnson JE, García-Herrera R. 2024. Climate Change Attribution of Extreme Events Using AI-Based Weather Models. EMS2024-280. In: European Meteorological Society (EMS) Annual Meeting 2024. Available at: https://meetingorganizer.copernicus.org/EMS2024/EMS2024-280.html (accessed 13 November 2024).

Kanae S, Oki T, Kashida A. 2004. Changes in hourly heavy precipitation at Tokyo from 1890 to 1999. Journal of the Meteorological Society of Japan Series II 82: 241-247. https://doi.org/10.2151/jmsj.82.241

Kheloufi-Attou A, Baba-Hamed K, Bouanani A. 2023. Homogénéisation des séries pluviométriques dans le cadre de l'évaluation de la Sécheresse 1982-2022 (Nord-Algérien). International Journal Water Science and Environment Technologies 8: 6-16.

Kim J, Porter J, Kearns EJ. 2023. Exposure of the US population to extreme precipitation risk has increased due to climate change. Scientific Reports 13: 21782. https://doi.org/10.1038/s41598-023-48969-7

Knutson T, Camargo SJ, Chan JCL, Emanuel K, Ho C-H, Kossin J, Mohapatra M, Satoh M, Sugi M, Walsh K, Wu L. 2020. Tropical cyclones and climate change assessment. Part II: Projected response to anthropogenic warming. Bulletin of the American Meteorological Society 101: E303-E322. https://doi.org/10.1175/BAMS-D-18-0194.1

Laborde JP, Gourbesville P, Assaba M, Demmak A, Belhouli L. 2010. Climate evolution and possible effects on surface water resources of North Algeria. Current Science 98: 1056-1062.

Meddi H, Meddi M. 2009. Variabilité des précipitations annuelles du Nord-Ouest de l'Algérie. Science et Changements Planétaires: Sécheresse 20: 57-65. https://doi.org/10.1684/sec.2009.0169

Meddi M, Toumi S. 2015. Spatial variability and cartography of maximum annual daily rainfall under different return periods in Northern Algeria. Journal of Mountain Science 12: 1403-1421. https://doi.org/10.1007/s11629-014-3084-3

Ndiaye A, Mbaye ML, Arnault J, Camara M, Lawin AE. 2023. Characterization of extreme rainfall and river discharge over the Senegal River basin from 1982 to 2021. Hydrology 10: 204. https://doi.org/10.3390/hydrology10100204

Nastos PT, Kapsomenakis J, Douvis KC. 2013. Analysis of precipitation extremes based on satellite and high-resolution gridded data set over Mediterranean basin. Atmospheric Research 131: 46-59. https://doi.org/10.1016/j.atmosres.2013.04.009

Nicholson SE, Nash DJ, Chase BM, Grab SW, Shanahan TM, Verschuren D, Asrat A, Lézine AM, Umer M. 2013. Temperature variability over Africa during the last 2000 years. The Holocene 23: 1085-1094. https://doi.org/10.1177/0959683613483618

Seneviratne SI, Zhang X, Adnan M, Badi W, Dereczynski C, Di Luca A, Ghosh S, Iskandar I, Kossin J, Lewis S, Otto F, Pinto I, Satoh M, Vicente-Serrano SM, Wehner M, Zhou B. 2021. Weather and Climate Extreme Events in a Changing Climate. In: Climate Change 2021: The Physical Science Basis. Contribution of Working Group I to the Sixth Assessment Report of the Intergovernmental Panel on Climate Change (Masson-Delmotte V, Zhai P, Pirani A, Connors SL, Péan C, Berger S, Caud N, Chen Y, Goldfarb L, Gomis MI, Huang M, Leitzell K, Lonnoy E, Matthews JBR, Maycock TK, Waterfield T, Yelekçi O, Yu R, Zhou B, Eds.). Cambridge University Press, New York, 1513-1766. https://doi.org/10.1017/9781009157896.013

Taïbi S, Meddi M, Mahé G. 2019. Seasonal rainfall variability in the southern Mediterranean border: Observations, regional model simulations and future climate projections. Atmósfera 32: 39-55. https://doi.org/10.20937/atm.2019.32.01.04

Von Mises R. 1936. La distribution de la plus grande de n valeurs. Revue Mathématique de l'Union Interbalkanique 1: 141-160.

WMO. 2009. Guidelines on analysis of extremes in a changing climate in support of informed decisions for adaptation (Klein Tank AMG, Zwiers FW, Zhang X, Eds.). WMO/TD-No. 1500. World Meteorological Organization, Geneva. Available at: https://library.wmo.int/idurl/4/48826 (accessed 9 June 2024).

Supplementary material

Table SI. List of rainfall stations used in the study.

Station	Geographic coordinates				Statistical description (mm)				
	Code	Latitude	Longitude	Z (m)	Average	Max	Min	SD	CV
Ain Oussara	S1	35.53º N	2.87º E	697	269.77	502.00	64.60	100.19	37.14
Ain Sefra	S2	32.77º N	–0.60º W	1059	152.17	362.10	30.00	72.33	47.53
Annaba	S3	36.82º N	7.81º E	5	610.51	925.00	326.00	134.66	22.06
Arzew	S4	35.82º N	–0.27º W	4	270.69	413.20	138.70	67.17	24.81
Batna	S5	35.55º N	6.18º E	1052	280.35	590.40	128.70	91.65	32.69
Beni Saf	S6	35.30º N	–1.35º W	70	285.80	452.30	53.60	94.67	33.12
Biskra	S7	34.85º N	5.72º E	38	125.40	344.30	41.50	69.89	55.73
Bordj Bou Arreridj	S8	36.07º N	4.77º E	930	333.97	542.20	159.30	84.40	25.27
Bou Chekif	S9	35.34º N	1.46º E	989	409.11	647.10	213.60	98.79	24.15
Bou Saâda	S10	35.33º N	4.21º E	461	150.15	220.20	86.30	36.33	24.20
Cheliff	S11	36.21º N	1.33º E	141	432.44	648.00	188.30	99.19	22.94
Constantine	S12	36.28º N	6.62º E	690	462.14	758.70	207.20	131.23	28.40
Dar El Beida (Alg)	S13	36.72º N	3.25º E	7	586.27	885.00	270.20	156.84	26.75
Djelfa	S14	34.68º N	3.25º E	1144	275.85	471.10	91.40	77.01	27.92
El Bayadh	S15	33.68º N	1.00º E	1347	264.57	545.70	103.00	94.79	35.83
El Kheiter	S16	34.15º N	0.07º E	1001	241.43	440.80	96.60	64.36	26.66
Es Senia (Oran)	S17	35.62º N	–0.62º W	90	326.57	544.90	187.60	89.48	27.40
Ghriss	S18	35.21º N	0.15º E	514	391.10	719.40	183.60	101.36	25.92
Jijel	S19	36.80º N	5.87º E	10	1016.0	1347.4	538.70	185.45	18.25
Maghnia	S20	34.82º N	–1.78º W	426	274.31	481.00	158.90	68.70	25.04
Mecheria	S21	33.54º N	–0.24º W	1175	198.48	410.80	42.30	73.63	37.10
Miliana	S22	36.30º N	2.23º E	721	773.43	1150.3	417.40	157.69	20.39
Mostaghanm	S23	35.88º N	0.12º E	138	212.07	313.80	96.60	51.03	24.06
M'Sila	S24	35.66º N	4.50º E	442	171.96	244.50	118.50	28.08	16.33
Oum El Bouaghi	S25	35.88º N	7.12º E	891	345.67	629.90	114.90	104.98	30.37
Relizane	S26	35.73º N	0.55º E	75	204.95	341.90	105.60	50.88	24.83
Saida	S27	34.87º N	0.15º E	752	305.58	481.10	153.60	75.78	24.80
Setif (Ain Arnat)	S28	36.18º N	5.32º E	1050	374.09	588.90	175.50	77.12	20.61
Skikda	S29	36.93º N	6.95º E	7	686.86	965.70	329.50	140.99	20.53
Soummam	S30	36.71º N	5.07º E	7	718.94	1372.8	258.30	203.98	28.37
Tébessa	S31	35.43º N	8.12º E	811	355.11	561.70	190.80	89.50	25.20
Zenata	S32	35.02º N	–1.45º W	248	302.27	473.60	124.30	78.99	26.13

Z: altitude; SD: standard deviation; CV: coefficient of variation.